Korean J. Chem. Eng., 40(1), 97-103 (2023)
DOI: 10.1007/s11814-022-1319-5

pISSN: 0256-1115
eISSN: 1975-7220

Characteristics of La-doped Pt/Al_2O_3 catalyst prepared by solvent-deficient method and effect on enhancement of dehydrogenation of perhydrodibenzyltoluene

Tae In Park[*], **Seong Ho Lee**[*,**,†], **and Kwan-Young Lee**[*,**,†]

*Department of Chemical and Biological Engineering, Korea University, 145, Anam-ro, Seongbuk-gu, Seoul 136-701, Korea
**Super Ultra Low Energy and Emission Vehicle Center, Korea University, 145, Anam-ro, Seongbuk-gu, Seoul 136-701, Korea

(*Received 26 September 2022 • Revised 16 October 2022 • Accepted 19 October 2022*)

Abstract−Liquid organic hydrogen carrier (LOHC) materials have been under the spotlight for the storage, transport and extraction of hydrogen. In particular, the catalytic process for extracting hydrogen from LOHC requires a fairly high level of catalytic technology due to several important issues, such as saving energy consumption due to endothermic reaction, minimizing consumption of LOHC for recycle, and high purity of hydrogen produced. This study focused on the development of La-doped Pt/Al_2O_3 catalyst with high activity for the dehydrogenation of perhydrodibenzyltoluene (H_{18}-DBT), which is well-known as a LOHC compound. The dehydrogenation performance of the La-doped Pt/Al_2O_3 catalyst was different depending on the La content it contained. A variety of characterization techniques are used to identify the performance differences of the catalysts. As revealed by the analyses of chemisorption, TEM and XPS, the number of lanthanum oxide particles on the surface of the catalyst increases and block the active sites of platinum, as the amount of La doped in the catalyst increases. However, by donating electrons from lanthanum oxide to platinum, the activity per unit active site of Pt increases. The Pt/La-Al_2O_3 catalyst doped with 1 wt% La showed much higher activity than that of the Pt/Al_2O_3, and showed the best performance among the catalysts doped with various amounts of La. In addition, it was found through spin-lattice relaxation analysis that La doping by solution-deficient method did not have a positive effect on the Pt dispersion by creating $Al^{3+}{}_{penta}$ sites inside the alumina particle rather than on the surface.

Keywords: Liquid Organic Hydrogen Carrier (LOHC), Dehydrogenation, Dibenzyltoluene, Pt/Al_2O_3, La-doped Al_2O_3, Solvent-deficient Method

INTRODUCTION

Power generation by renewable energy is inherently intermittent, so the advanced technology of energy storage should be combined to use it effectively. Since most of energy storage technologies have low density, low capacity, and high cost, the chemical storage methods using hydrogen have been studied and, recently, hydrogen storage using liquid organic hydrogen carrier (LOHC) is known as a promising technology [1-4].

LOHC can store hydrogen inside a molecule and reversibly release hydrogen. It is classified into a heterocyclic compound containing heteroatoms such as nitrogen and boron, and a homocyclic compound containing no heteroatom [1,4-6]. LOHC materials containing heteroatoms have low dehydrogenation temperature due to low dehydrogenation enthalpy, but have low stability in dehydrogenation reaction, high material cost, and toxicity [5,6].

Dibenzyltoluene (DBT) has a hydrogen storage capacity of 6.2 wt%, which meets the standards required by the U. S. Department of Energy (DOE) [1,7]. In addition, since it has been commercialized as a heat transfer fluid, it has high thermal stability, and also satisfies other factors to be verified for commercialization of LOHC, such as material stability, harm to the human body, and securing a container [1,7]. The hydrogenation reaction of dibenzyltoluene (DBT) proceeds at a high conversion rate at a low temperature, whereas the dehydrogenation of perhydrodibenzyltoluene (H_{18}-DBT) is thermodynamically endothermic and proceeds at a relatively high temperature [1]. However, the high reaction temperature for dehydrogenation may lower the efficiency of an energy storage system and cause side reactions to lower the purity of hydrogen [1,8,9]. Therefore, it is necessary to develop a highly active dehydrogenation catalyst in order to lower the reaction temperature and suppress side reactions.

The catalyst used for the dehydrogenation of H_{18}-DBT is mainly known as a platinum-alumina catalyst [1,9-11]. Alumina is widely used as a catalyst support due to its excellent stability and surface properties favorable for catalytic reaction [12]. In particular, γ-Al_2O_3, a kind of transitional alumina, has a large specific surface area [12], and is known to interact strongly with barium oxide [13] and platinum [14-16] at the $Al^{3+}{}_{penta}$ site that is not coordinatingly saturated. Therefore, it can be advantageous for the synthesis of a platinum catalyst having a high degree of dispersion.

On the other hand, a study on the dehydrogenation of H_{18}-DBT using a metal-doped Pt/Al_2O_3 catalyst has been reported [17]: Pt/Mg-Al_2O_3 catalyst showed improved performance compared to the Pt/Al_2O_3 and Pt/Zn-Al_2O_3 catalysts, and the superior activity of the Pt/Mg-Al_2O_3 catalyst was due to the increased concentration of electron-rich Pt species on the Mg-modified catalyst surface. However, in the reported study, the characterization analysis of Pt and Mg on the catalyst surface is insufficient, so further stud-

---

[†] To whom correspondence should be addressed.
E-mail: seongholee@korea.ac.kr, kylee@korea.ac.kr

ies are needed. Similar to Mg in the reported study, lanthanum is known as an alkaline metal [18], and there is a study that the number of Al^{3+}_{penta} sites increases when alumina is modified with lanthanum [19].

In this study, the La-doped Pt/Al_2O_3 catalysts with various La doping contents were studied with the intention of the electron donating effect of alkaline metal and the high dispersion effect of Pt by the increased number of Al^{3+}_{penta} sites. As the La doping method, the solvent-deficient method capable of doping La at the same time as synthesizing alumina was used. It is known that by using the solvent-deficient method, alumina having a structure similar to that prepared by the sol-gel method can be prepared and the time and cost required for the synthesis can be reduced [20,21]. In addition, various characterization analyses, such as chemisorption, TEM, ^{27}Al-NMR, and spin-lattice relaxation, were performed to investigate the factors that mainly affect the activity of the La-doped Pt/Al_2O_3 catalyst for the dehydrogenation of H_{18}-DBT.

EXPERIMENTAL METHODS

1. Support Synthesis

Alumina with various doping amounts of La was synthesized by using the solvent-deficient method [20]. An appropriate amount of lanthanum(III) nitrate hexahydrate (Sigma-Aldrich) was dissolved in deionized water. The prepared solution and aluminum iso-propoxide (Sigma-Aldrich) were mixed in a mortar for 20 minutes. The molar ratio of water to aluminum was 5 : 1 and the amount of lanthanum corresponded to 0, 1, 2, 4, and 8% by weight of alumina. After mixing, the resulting white intermediate was heated to 600 °C at a ramping rate of 2 °C/min in air, and then maintained at 600 °C for 4 hours. The synthesized alumina was expressed as xLa-Al_2O_3 (x is wt%, x=0, 1, 2, 4, 8) according to the doping amount of La.

2. Catalyst Synthesis

The Pt/La-Al_2O_3 catalysts were synthesized using the incipient wetness method. The appropriate amount of chloroplatinic acid hydrate (Sigma-Aldrich) was dissolved in deionized water. After the prepared solution was added dropwise to the La-Al_2O_3 powder, the wet sample was dried at 120 °C overnight. The dried sample was heated to 300 °C with a ramping rate of 2 °C/min in air, and then maintained at 300 °C for 2 hours. Finally, the prepared catalyst was reduced at 300 °C for 2 hours in a 10 mol% H_2/Ar atmosphere before reaction.

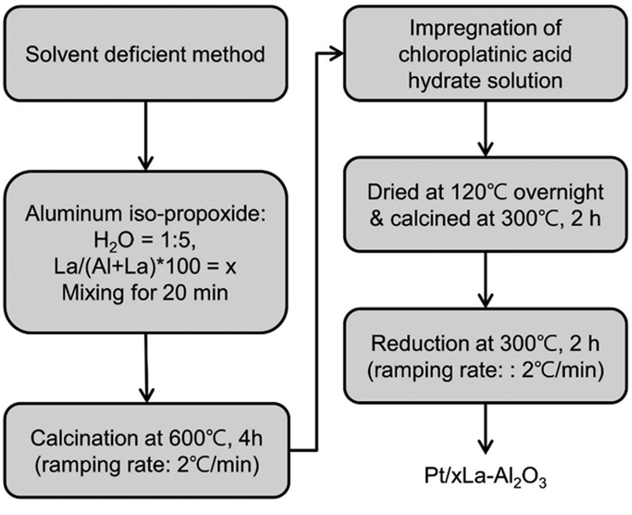

Fig. 1. Synthesis procedures of La-Al_2O_3 and Pt/La-Al_2O_3.

The catalyst used in the preliminary experiments to confirm the optimal loading of platinum was synthesized using the same process except for the amount of chloroplatinic acid hydrate.

3. Characterization and Activity Test

The sample crystallinity was measured by powder X-ray diffraction (XRD). The samples were analyzed using D/MAX-2500/PC (Rigaku) at the Korean Institute of Science and Technology (KIST). XRD patterns were collected from 10° to 90° with a scanning rate of 1°/min using Cu Kα radiation (λ=1.5418 Å).

The texture properties of the supports were determined from N_2 adsorption/desorption measurement at −196 °C using BELSORP-MAX (Bell Japan, Inc.). The samples were degassed at 150 °C under vacuum conditions overnight to remove moisture. Specific surface area and pore volume were calculated by the Brunauer-Emmet-Teller (BET) method. Pore size distribution of the samples was calculated by the Barrett-Joyner-Halenda (BJH) method using the desorption branch.

^{27}Al NMR analysis was conducted at National Center for Inter-University Research Facilities (NCIRF). A chemical shift of aluminum and spin-lattice relaxation time (T_1) were measured using 500 MHz Avance III HD (Bruker) instrument.

Temperature-programmed desorption of ammonia (NH_3-TPD) was conducted with a BELCAT (BEL Japan, Inc.) instrument. Before measurement, the samples were pretreated in the apparatus at 500 °C for 1 hour in He atmosphere to remove moisture and other residues. Ammonia was adsorbed on the sample surface at 100 °C for 30 minutes. Then, the sample temperature was increased from 100 °C to 800 °C under a flow of He. The desorbed ammonia was detected with a thermal conductivity detector (TCD).

The dispersion of Pt particles on the catalyst was measured using CO chemisorption on Autochem II (Micromeritics). Prior to analysis, the sample was reduced at 300 °C for 2 hours inside the instrument. CO was adsorbed at 50 °C for 10 minutes in an 8% CO/He atmosphere. The metallic dispersion was calculated using the following equation assuming that the adsorption stoichiometry of CO and Pt was 1.

$$\text{Dispersion } (D_{CO}, \%) = \frac{\text{Quantity of adsorbed CO (mol)}}{\text{Total amount of Pt (mol)}} \times 100$$

The chemical composition and oxidation state of the samples were analyzed using X-ray photoelectron spectroscopy (XPS). The XPS measurement was conducted using AXIS-NOVA (Kratos Inc.) instrument at Korea Basic Science Institute (KBSI). The C 1s, Al 2p, Pt 4d, La 3d spectra were measured and the binding energies were referenced using the C 1s at 284.8 eV. Prior to measurement, samples were preserved under a vacuum.

The structure of the catalysts was analyzed by transmission electron microscopy (TEM; JEM-ARM200F, JEOL Ltd.) at the National Center for Inter-University Research Facilities (NCIRF). The catalyst samples were dispersed in methanol and the diluted samples were dropped onto copper grids. The sample grids were dried in an oven at 80 °C in vacuum overnight.

4. Catalytic Activity Tests

The hydrogenation of DBT was performed by using a batch-type autoclave reactor (4598 Micro Reactor, Parr Instrument) [1]. A 30 g of DBT and 0.557 g Ru/Al_2O_3 (5 wt%, Sigma-Aldrich) catalyst corresponding to a molar ratio of 0.25 mol% (Ru/DBT) were loaded in the reactor. To remove air and moisture, the reactor was purged several times with H_2. After flushing, the reactor was pressurized to 50 bar and heated to 150 °C using a heating jacket. The hydrogenation reaction was performed at 150 °C for 3.5 hours with stirring at 1,000 rpm. The purity of H_{18}-DBT was analyzed using gas chromatography-mass spectroscopy (GC-MS) [11].

The dehydrogenation reactions were performed in a batch-type reactor [1]. A 5 g of H_{18}-DBT and catalyst corresponding to a molar ratio of 0.15 mol% (Pt/H_{18}-DBT) were added to a 50 ml three-neck glass flask. The reactor was purged with 100 sccm of N_2 for 10 minutes to remove air. After flushing, the reactor was heated to 270 °C with stirring at 1,000 rpm. The dehydrogenation process was performed for 3.5 hours at 270 °C. The released H_2 was measured with a mass flow meter (MFM) using 15 sccm of N_2 as carrier gas. The degree of dehydrogenation was calculated using the following equation:

$$\text{Degree of dehydrogenation (\%)} = \frac{\text{Quantity of evolved hydrogen (mol)}}{\text{Quantity of hydrogen in reactants (mol)}} * 100$$

The turnover frequency (TOF), which represents the efficiency of exposed active sites, was calculated using the following equation. Exposed platinum sites were calculated by using the CO chemisorption:

$$\text{TOF} = \frac{\text{Quantity of evolved hydrogen (mol)}}{\text{Exposed platinum in catalysts (mol)} \times \text{time (hour)}}$$

RESULTS AND DISCUSSION

Prior to the study of activity enhancement according to La doping into Pt/Al_2O_3, an experiment was performed to confirm the optimal loading amount of platinum for the dehydrogenation reaction. Fig. 2 shows the activity results of platinum catalysts with different Pt loadings for the dehydrogenation of H_{18}-DBT. Dehydrogenation activity was improved with increasing platinum loading up to 5 wt%, and then decreased at 10 wt%. Based on these results, assuming that the loading amount of 5 wt% is roughly suitable for the dehydrogenation reaction of H_{18}-DBT, subsequent experiments were performed by loading 5 wt% Pt on La-doped alumina.

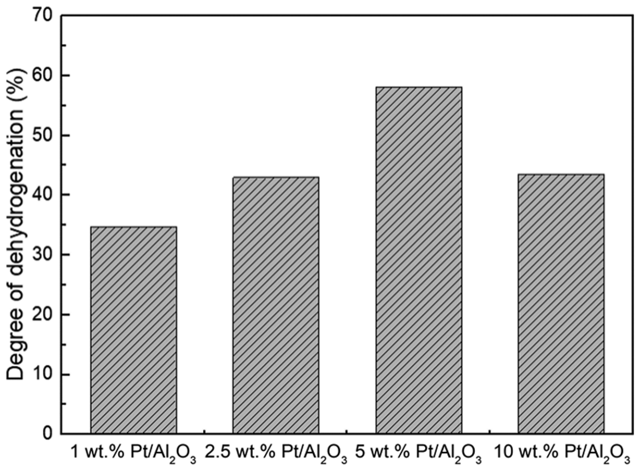

Fig. 2. Catalytic activity of Pt/Al_2O_3 catalysts with different Pt loadings for H_{18}-DBT dehydrogenation.

1. Structural Analysis

XRD analysis was performed to analyze the crystal phases of La-Al_2O_3 materials with various La contents prepared by the solvent-deficient method, and the results are shown in Fig. 3. It was confirmed that the intensity of the (400) and (440) planes of γ-Al_2O_3 decreased as the content of La in the alumina increased. In addition, it was confirmed that the crystalline phase of γ-Al_2O_3 almost disappeared in the sample having a weight of 8% La, and the crystalline phase corresponding to lanthanum aluminate was observed instead. From the results, it was found that the presence of lanthanum during alumina synthesis weakens the formation of γ-Al_2O_3 crystals, and the presence of a certain amount or more of lanthanum suppresses the crystallization of γ-Al_2O_3 completely.

To confirm the textural properties of the synthesized La-Al_2O_3 materials according to the La content, specific surface area and pore distribution analysis were performed, and the results are shown in Table 1 and Fig. 4. As can be seen from Fig. 4, the pores corresponding to the diameter range of 10-20 nm were observed in most samples except for 8La-Al_2O_3. As the content of La in the sample increased, the pore volume of the sample gradually decreased, and

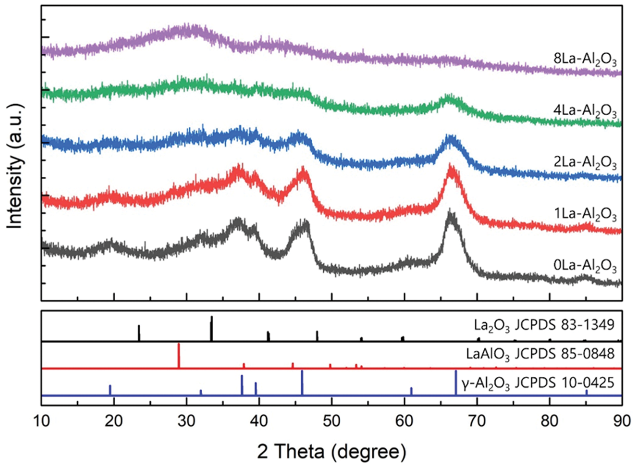

Fig. 3. XRD spectra of La-Al_2O_3 materials with various La contents prepared by the solvent-deficient method.

Table 1. Pore volume and specific surface area of synthesized La-Al_2O_3 samples

Sample	Pore volume (mL/g)	Surface area (m^2/g)
0La-Al_2O_3	1.85	324
1La-Al_2O_3	1.82	341
2La-Al_2O_3	1.67	347
4La-Al_2O_3	1.41	311
8La-Al_2O_3	1.06	144

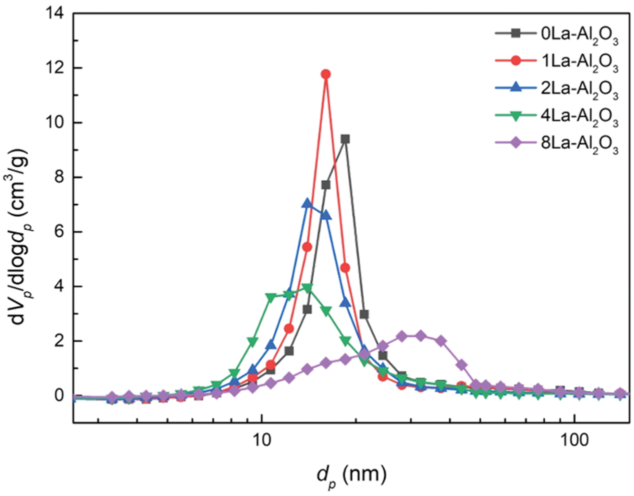

Fig. 4. Pore size distribution of synthesized La-Al_2O_3 samples.

in 8La-Al_2O_3, pores of any other diameter, including pores with a size of 10-20 nm, were not observed. Consistent with these results, it can be seen that the specific surface area and pore volume decreased as the La content increased, and the specific surface area was significantly reduced in 8La-Al_2O_3. Therefore, in the case of La-Al_2O_3 prepared by the solvent-deficient method, the γ-Al_2O_3 crystal phase is suppressed as the La content is increased, and the particles are contracted so that the pore structure and specific surface area are not developed.

2. Catalytic Activity

Fig. 5 shows the activity of the catalysts with various La content. The 5Pt/1La-Al_2O_3 catalyst doped with 1 wt% of La had the highest activity, which is a result of 9% improvement compared to the catalyst without La doping. As the content of La increased from 1 wt% to 4 wt%, the activity of the corresponding catalyst decreased in inverse proportion, and the 5Pt/4La-Al_2O_3 catalyst doped with 4 wt% of La showed lower activity than the 5Pt/0La-Al_2O_3 catalyst without doping.

The Al^{3+}_{penta} site on the surface of γ-Al_2O_3 is known to strongly interact with barium oxide [13] and platinum [14]. In addition, it has been reported that when a mixed oxide is formed by doping La into alumina, the Al^{3+}_{penta} site is greatly increased [19]. Therefore, logically, it is expected that the Al^{3+}_{penta} sites of γ-Al_2O_3 increase with the doping amount of La, and the catalytic activity increases due to the high dispersion of Pt.

Meanwhile, Garidzirai et al. reported a study on the catalyst development in the same reaction system as this study [17]. The authors claim that the dehydrogenation activity is improved by increasing the metallic Pt concentration on the catalyst surface when the Pt/Al_2O_3 catalyst is modified with Mg as a co-catalyst, but it is thought that the evidence presented through direct analysis of the catalyst is somewhat insufficient.

As such, the activity of the catalyst according to the amount of La doping may be affected by various variables, including the degree of dispersion and the electronic state of Pt. Therefore, various analyses were performed to clarify the reason for the difference in catalytic activity.

3. Pt Dispersibility

3-1. NMR Analysis

^{27}Al NMR analysis was performed to confirm how the Al^{3+}_{penta} site in alumina changes with La doping, and it is shown in Fig. 6. The three peaks located at 8, 36, and 67 ppm correspond to the Al^{3+}_{octa} site, Al^{3+}_{penta} site, and Al^{3+}_{tetra} site, respectively [14]. In general, it is known that Al^{3+}_{octa} sites and Al^{3+}_{tetra} sites occupy most of γ-Al_2O_3, and the ratio of Al^{3+}_{penta} sites is relatively small [13]. Also, the Al^{3+}_{penta} site is generated by the change of the Al^{3+}_{octa} site, and it is known to be unstable because it is not coordinatively saturated [13,14]. As can be seen in Fig. 5, as the amount of La doped in alumina increases, the ratio of Al^{3+}_{penta} sites increases. This is thought to be because the increase in Al-O-La bonds in γ-Al_2O_3 induced the generation of Al^{3+}_{penta} sites corresponding to defect sites. Assuming that such an increase in Al^{3+}_{penta} site can increase metal dispersion and increase activity, the 5Pt/2La-Al_2O_3 and 5Pt/4La-Al_2O_3 catalysts evaluated in this study should show higher activity. However, the catalyst performance of 5Pt/1La-Al_2O_3 was the best, and the 5Pt/4La-Al_2O_3 catalyst had lower dehydrogenation performance than the 5Pt/0La-Al_2O_3 catalyst without La, so additional analysis

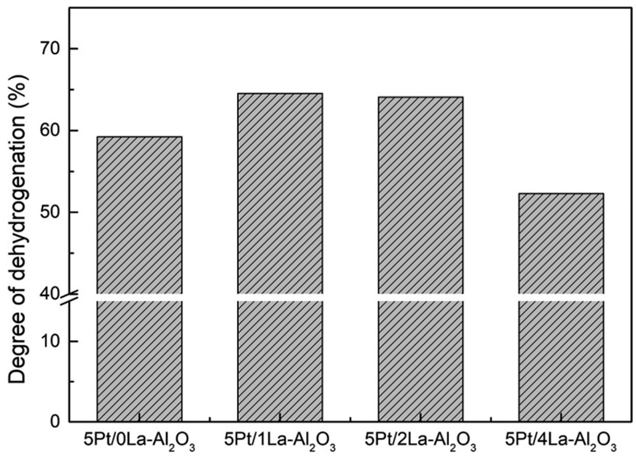

Fig. 5. Catalytic performance of the 5Pt/La-Al_2O_3 catalysts for H_{18}-DBT dehydrogenation.

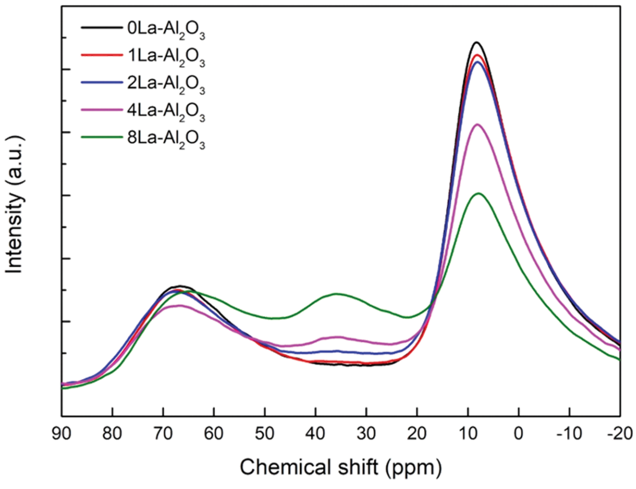

Fig. 6. ^{27}Al NMR analysis results of La-Al_2O_3 materials.

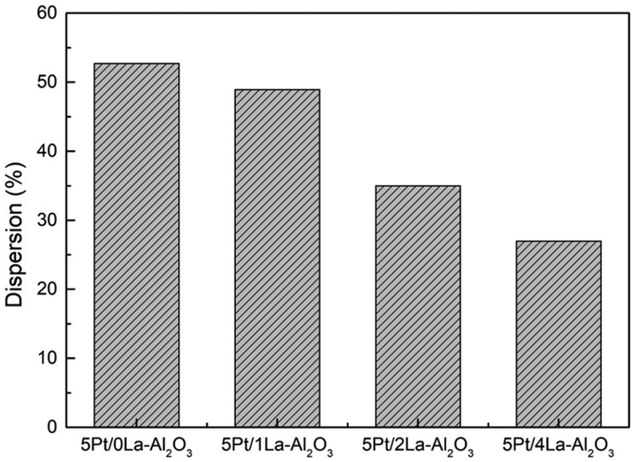

Fig. 7. Pt dispersion of 5Pt/La-Al_2O_3 materials analyzed by CO chemisorption.

was needed to explain these results.

3-2. Chemisorption Analysis

In the La-Al_2O_3 materials prepared in this study, it was confirmed that the amount of Al^{3+}_{penta} sites increased in proportion to the doped La content. Therefore, CO chemisorption analysis was performed to confirm the change in platinum dispersion of the prepared catalyst according to the change in the amount of Al^{3+}_{penta} site, and the results are shown in Fig. 7. The analysis confirmed that the dispersion degree was rather linearly decreased as the doped La content was increased. This is contrary to the results of previous studies that the Al^{3+}_{penta} site on the surface of the support can increase the dispersion by acting as an anchoring site for platinum [14,16,22]. Therefore, it can be assumed that the size of the Pt particles on the catalyst surface increases proportionally as the amount of La doping increases, or otherwise, the doped La particles gradually cover the surface of the Pt particles. One of these assumptions is made clearer by spin-lattice relaxation analysis and TEM analysis.

3-3. Spin-lattice Relaxation Analysis

The 4La-Al_2O_3 prepared by the solvent-deficient method showed the highest Al^{3+}_{penta} site strength among the catalysts used for activity evaluation, as previously confirmed through NMR. However, the enhanced amount of Al^{3+}_{penta} sites in the La-Al_2O_3 material did not have a positive effect on the dispersion of platinum in the catalyst prepared using it. For the Al^{3+}_{penta} site to act as an anchoring site for Pt, the Al^{3+}_{penta} site must be located on the surface [13]. Therefore, through spin-lattice relaxation analysis of the 4La-Al_2O_3 sample, it was attempted to determine whether Al^{3+}_{penta} sites exist on the surface of the support, and the result is shown in Fig. 8.

When Al^{3+}_{penta} sites exist on the surface of the La-Al_2O_3 materials, the relaxation time (T_1) of Al^{3+}_{penta} sites should measure faster than the spin-lattice relaxation time of Al^{3+}_{octa} sites and Al^{3+}_{tetra} sites [13]. However, it was confirmed that the relaxation time (T_1) of the Al^{3+}_{penta} site measured more slowly than the spin-lattice relaxation time of the Al^{3+}_{octa} site and the Al^{3+}_{tetra} site. That is, in the case of La-doped Al_2O_3 prepared by the solvent-deficient method in this study, most of the Al^{3+}_{penta} sites induced by lanthanum doping exist inside, not on the surface of γ-Al_2O_3 particle. Therefore, it is interpreted that the enhanced amount of Al^{3+}_{penta} sites in the La-Al_2O_3 material did not affect the Pt dispersion of the catalyst.

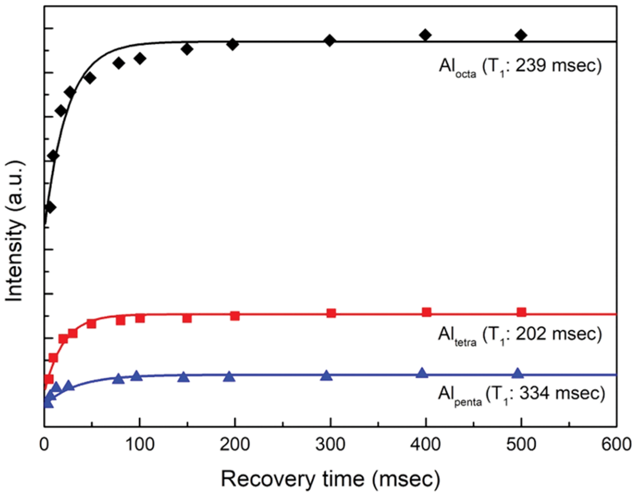

Fig. 8. Spin-lattice relaxation measurement result of 4La-Al_2O_3.

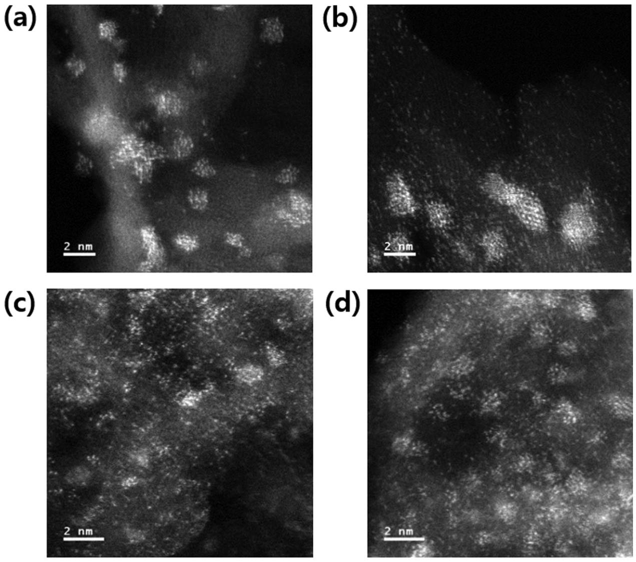

Fig. 9. STEM images of (a) 5Pt/0La-Al_2O_3, (b) 5Pt/1La-Al_2O_3, (c) Pt/2La-Al_2O_3, and (d) 5Pt/4La-Al_2O_3.

3-4. TEM Analysis

Fig. 9 shows the scanning transmission electron microscopy (STEM) images of the catalysts prepared in this study. Fig. 9(a) is an image of Pt particles supported on 0La-Al_2O_3 not including lanthanum, and the size of the Pt particles was identified as about 1.5 nm on average. The particle size does not seem to change significantly regardless of the La doping amount, whereas as the La doping amount increases, more small and fine particles presumed to be lanthanum oxide are conspicuous. Therefore, in the CO chemisorption results, the decrease in Pt dispersion as the amount of La doping increased cannot be attributed to the increase in Pt particle size. In addition, it is reasonable to interpret that the doped La was partially exposed to the alumina surface, and then the lanthanum oxide particles covered the surface of the Pt particles to

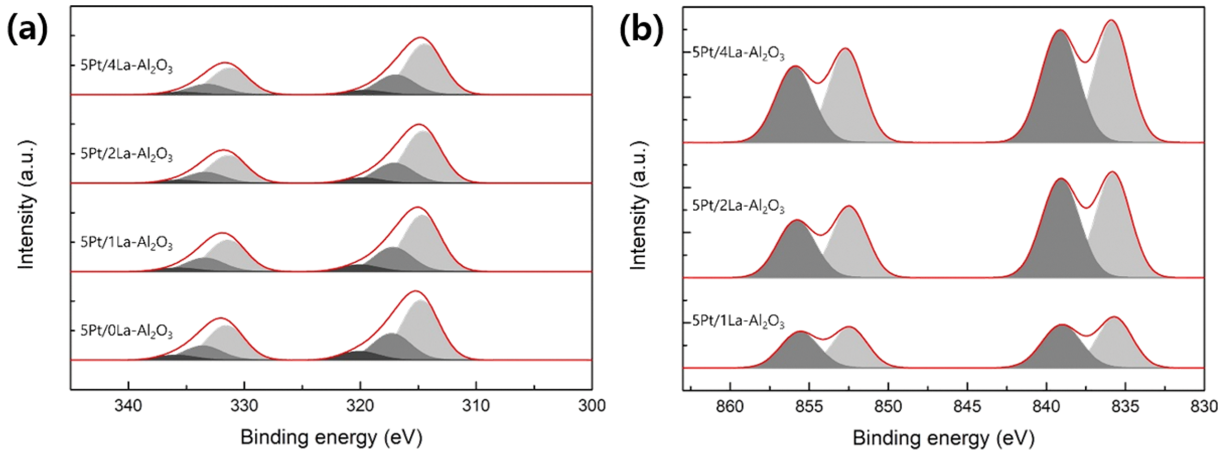

Fig. 10. (a) Pt 4d and (b) La 3d XPS spectra of 5Pt/La-Al$_2$O$_3$ catalysts.

Table 2. Pt 4d binding energies of 5Pt/La-Al$_2$O$_3$ catalysts

	Binding energy (eV)					
	Pt 4d$_{5/2}$			Pt 4d$_{3/2}$		
	Pt^0	Pt^{2+}	Pt^{4+}	Pt^0	Pt^{2+}	Pt^{4+}
5Pt/0La-Al$_2$O$_3$	314.80	317.30	320.10	331.60	333.60	335.90
5Pt/1La-Al$_2$O$_3$	314.66	317.19	320.06	331.44	333.43	335.75
5Pt/2La-Al$_2$O$_3$	314.59	317.10	319.80	331.38	333.39	335.69
5Pt/4La-Al$_2$O$_3$	314.45	316.97	319.65	331.26	333.25	335.57

Table 3. La 3d binding energies of 5Pt/La-Al$_2$O$_3$ catalysts

Catalysts	Binding energy (eV)			
	La 3d$_{5/2}$		La 3d$_{3/2}$	
5Pt/1La-Al$_2$O$_3$	835.66	839.05	852.42	855.62
5Pt/2La-Al$_2$O$_3$	835.77	839.11	852.45	855.83
5Pt/4La-Al$_2$O$_3$	835.84	839.17	852.66	855.94

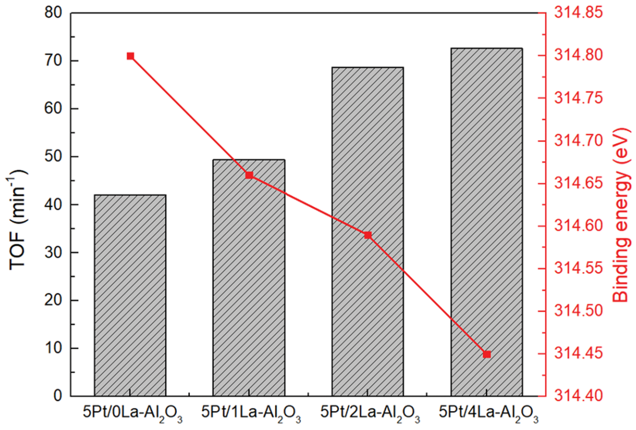

Fig. 11. TOF and Pt 4d binding energies of 5Pt/La-Al$_2$O$_3$ catalysts.

prevent the adsorption of CO in the chemisorption analysis.

4. Pt Reducibility (XPS Analysis)

XPS analysis was performed to confirm the electronic states of the surface elements of each catalyst, and the results are shown in Fig. 10, Tables 2 and 3.

In the case of Pt, the Al 2p signal and the Pt 4f signal were overlapped to analyze the Pt 4d region, and in the case of La, La 3d was analyzed. The peaks located at 314.8 eV and 331.6 eV correspond to 4d5/2 Pt^0 and 4d$_{3/2}$ Pt^0, respectively. In addition, the peaks located at 317.3 eV and 333.6 eV correspond to 4d$_{5/2}$ Pt^{2+} and 4d$_{3/2}$ Pt^{2+}, respectively, and the peaks at 320.1 eV and 335.9 eV correspond to 4d$_{5/2}$ Pt^{4+} and 4d$_{3/2}$ Pt^{4+}, respectively. The peak located at 835.7 eV and 839.1 eV correspond to La 3d$_{5/2}$, and the peaks at 852.4 eV and 855.6 eV correspond to La 3d$_{3/2}$, respectively.

As can be seen more clearly from Table 2 and 3, the higher the doped La content in the catalyst, the lower the binding energy of each region of platinum. In addition, in the case of lanthanum, it was confirmed that the binding energy increased as the amount of La doping increased. Therefore, it can be seen that the lanthanum oxide present on the surface of Pt donates electrons to Pt, so that the electron density of Pt increases and the electron density of lanthanum decreases. According to a previously published study on the dehydrogenation reaction of H$_{18}$-DBT, the change in the electron density of Pt has a great effect on the dehydrogenation activity, and it is known that the dehydrogenation activity can be improved when the electron density of Pt is increased [17,23-25].

Considering the results of various catalyst characterization analyses, it was found that as the amount of La doping increased, the number of active sites in Pt decreased, which negatively affected the activity, but the electron density of Pt increased and thus had a positive effect on the activity. Therefore, an optimal La doping amount may exist and, in this study, it was estimated to be about 1 wt%.

To highlight the relationship between the electron density of Pt and the H_{18}-DBT dehydrogenation activity, the turnover frequency (TOF) values and the Pt 4d binding energy values of catalysts are shown together in Fig. 11. The TOF values of the catalysts are inversely proportional to the Pt binding energy values of the catalysts, and it can be confirmed that electron donation of La to Pt in the dehydrogenation reaction is a major factor increasing the activity of the catalyst.

CONCLUSIONS

This study investigated the effect of La doping and doping amount to the Pt/Al_2O_3 catalyst on the catalytic activity for the dehydrogenation of H_{18}-DBT. In addition, a simple and economical solvent-deficient method was applied when synthesizing La-doped alumina, and the effect of La doping to alumina by this synthesis method was also studied.

The results derived from this study are as follows;

- In La-Al_2O_3 prepared by the solvent-deficient method, it was confirmed that La mainly creates Al^{3+}_{penta} sites inside the particle rather than on the surface of alumina particle.
- La exposed on the surface of alumina covered the Pt particles in the form of oxide to reduce the reaction sites, and at the same time increased the activity per unit reaction site by donating electrons to Pt.
- The effect of electron donation of La to Pt on the enhancement of catalytic performance for the dehydrogenation reaction of H_{18}-DBT is major enough to outweigh the disadvantage of sacrificing a certain reaction site. 1 wt% La-doped Pt/La-Al_2O_3 catalyst showed the best performance for the dehydrogenation of H_{18}-DBT.

Finally, the Pt/La-Al_2O_3 catalyst developed in this study not only shows superior catalytic performance (about 9% increased) compared to the conventional Pt/Al_2O_3 catalyst in the dehydrogenation of H_{18}-DBT, but is also manufactured by a simpler and more economical manufacturing method. Therefore, it is expected to be applied to the catalytic dehydrogenation process of various LOHC compounds in the future.

ACKNOWLEDGEMENTS

This study was supported by a National Research Foundation of Korea (NRF) grant funded by the Korean Government (MSIP) (NRF-2019M3E6A1064876).

REFERENCES

1. N. Brückner, K. Obesser, A. Bösmann, D. Teichmann, W. Arlt, J. Dungs and P. Wasserscheid, *ChemSusChem*, **7**, 229 (2014).
2. S. Mekhilef, R. Saidur and A. Safari, *Phys. Chem. Chem. Phys.*, **16**, 981 (2012).
3. M. Felderhoff, C. Weidenthaler, R. von Helmolt and U. Eberle, *Phys. Chem. Chem. Phys.*, **9**, 2643 (2007).
4. D. Teichmann, W. Arlt, P. Wasserscheid and R. Freymann, *Energy Environ. Sci.*, **4**, 2767 (2011).
5. P. Preuster, C. Papp and P. Wasserscheid, *Acc. Chem. Res.*, **50**, 74 (2017).
6. P. C. Rao and M. Yoon, *Energies*, **13**, 6040 (2020).
7. P. Modisha and D. Bessarabov, *Sustain. Energy Fuels*, **4**, 4662 (2020).
8. M. S. Akhtar, R. Dickson and J. J. Liu, *ACS Sustain. Chem. Eng.*, **9**, 17152 (2021).
9. L. Shi, S. Qi, J. Qu, T. Che, C. Yi and B. Yang, *Int. J. Hydrogen Energy*, **44**, 5345 (2019).
10. A. Ali, A. K. Rohini, Y. S. Noh, D. J. Moon and H. J. Lee, *Int. J. Energy Res.*, **46**, 6672 (2022).
11. P. M. Modisha, J. H. Jordaan, A. Bösmann, P. Wasserscheid and D. Bessarabov, *Int. J. Hydrogen Energy*, **43**, 5620 (2018).
12. M. Trueba and S. P. Trasatti, *Eur. J. Inorg. Chem.*, **2005**, 3393 (2005).
13. J. H. Kwak, J. Z. Hu, D. H. Kim, J. Szanyi and C. H. Peden, *J. Catal.*, **251**, 189 (2007).
14. J. H. Kwak, J. Hu, D. Mei, C.-W. Yi, D. H. Kim, C. H. Peden, L. F. Allard and J. Szanyi, *Science*, **325**, 1670 (2009).
15. J. Lee, E. J. Jang, D. G. Oh, J. Szanyi and J. H. Kwak, *J. Catal.*, **385**, 204 (2020).
16. L. Shi, G. M. Deng, W. C. Li, S. Miao, Q. N. Wang, W. P. Zhang and A. H. Lu, *Angew. Chem. Int. Ed.*, **54**, 13994 (2015).
17. R. Garidzirai, P. Modisha, I. Shuro, J. Visagie, P. van Helden and D. Bessarabov, *Catalysts*, **11**, 490 (2021).
18. M. Sánchez-Sánchez, R. Navarro and J. Fierro, *Int. J. Hydrogen Energy*, **32**, 1462 (2007).
19. J. H. Song, S. Yoo, J. Yoo, S. Park, M. Y. Gim, T. H. Kim and I. K. Song, *Mol. Catal.*, **434**, 123 (2017).
20. B. Huang, C. H. Bartholomew, S. J. Smith and B. F. Woodfield, *Micropor. Mesopor. Mater.*, **165**, 70 (2013).
21. S. J. Smith, B. Huang, C. H. Bartholomew, B. J. Campbell, J. Boerio-Goates and B. F. Woodfield, *J. Phys. Chem. C*, **119**, 25053 (2015).
22. H. Jeong, O. Kwon, B.-S. Kim, J. Bae, S. Shin, H.-E. Kim, J. Kim and H. Lee, *Nat. Catal.*, **3**, 368 (2020).
23. C. H. Kim, M.-W. Lee, J. S. Jang, S. H. Lee and K.-Y. Lee, *Fuel*, **313**, 122654 (2022).
24. Y. Sugiura, T. Nagatsuka, K. Kubo, Y. Hirano, A. Nakamura, K. Miyazawa, Y. Iizuka, S. Furuta, H. Iki and T. Higo, *Chem. Lett.*, **46**, 1601 (2017).
25. X. Yang, Y. Song, T. Cao, L. Wang, H. Song and W. Lin, *Mol. Catal.*, **492**, 110971 (2020).